Modeling Abutment Contact-Friction Using Run-Time Parameter Updates

Asifur Rahman[a], Kevin R. Mackie[b], Michael H. Scott[c]

[a]*Civil Engineering, Stony Brook University, Stony Brook, 11794, NY, USA*
[b]*Civil, Env., and Construction Engineering, University of Central Florida, Orlando, 32816-2450, FL, USA*
[c]*Civil and Construction Engineering, Oregon State University, Corvallis, 97331, OR, USA*

Abstract

Nonlinear modeling of seat-type abutment behavior has evolved during response history analysis from simple linear elastic springs or single-point constraints to more refined models of bearing, back wall, shear key, and back fill contributions. While most longitudinal models consider the gap closure effect, only select few studies have looked at the different possible contact-friction responses that are generated, particularly in the case of skewed abutments. This paper presents nonlinear static and nonlinear dynamic results for several abutment and bridge scenarios based on a novel modeling approach developed by the authors. The Coulomb contact-friction interface (at several locations between the superstructure, back wall, and shear keys) is modeled using only linear elastic (or elastic-perfectly-plastic) springs that undergo user-driven run-time parameter updates during the analysis. The parameterization method was previously benchmarked against classical solutions from node-to-node contact literature, and in this paper is extended to studying the response of abutments in OpenSees. Results are presented for two simplified cases of rigid superstructures relative to results from the literature. The nonlinear static and dynamic behaviors of the abutment are then extended to response history analysis of standard reinforced concrete overpass bridges as compared with other common abutment modeling approaches. Results demonstrate scenarios where friction after contact changes the frequency response and therefore demand in the bridge system as well as when it may be neglected entirely.

1. Introduction

It has been long recognized, particularly for short- to medium-span bridges, that the boundary conditions at the abutment can play a significant role in the seismic response of bridges. Mackie et al. (2017) showed in some cases the boundary conditions (and parameters of the spring models used to describe abutment

This is a preprint and may be downloaded for personal use only. Published in the *18th World Conference on Earthquake Engineering (WCEE2024)*, and may be found at: https://proceedings-wcee.org/view.html?id=23274&conference=18WCEE

behaviour) drive the response sensitivity in nonlinear time history analysis. Aviram et al. (2008) found that using simplified abutment models caused major differences in the ultimate shear strength, displacements, mode shapes, and periods and that an appropriate abutment model is needed to correctly capture the global response. The effect of abutment modelling is therefore relevant for both performance-based assessment and performance-based design. A majority of performance-based earthquake engineering (PBEE) studies on bridges now conduct fragility analysis of bridge systems using nonlinear models and suites of ground motions. Therefore, there has been a need to calibrate not only the stiffness contributions from the different abutment components, but also the strength (Shamsabadi et al. (2005), Sextos et al. (2008), Taskari and Sextos (2012)). Although more refined three-dimensional (3D) continuum studies exist on abutments (Darwash and Mackie (2021)), they are usually limited to nonlinear static response due to complexities of calibrating cyclic multiaxial constitutive models and computational demands. A majority of nonlinear dynamic studies have utilized different levels of macro-model refinement (linear/nonlinear springs, gaps, dashpots). Macro-models have been used in a majority of nonlinear dynamic studies when investigating the effect of abutment-soil-structure interaction and embankment flexibility on the seismic response of the bridge system (Inel and Aschheim (2004), Kotsoglou and Pantazopoulou (2010)). Several studies have also identified the importance of frequency-dependent contributions to the stiffness and/or damping (Wilson (1988), Zhang and Makris (2002)). Specific to seat-type abutments in this paper, the primary abutment resistance is drawn from the shear keys, backwall, wingwalls, and corresponding backfill. Many previous models focused on the embankment flexibility (in all three principal directions) and the passive resistance of the backwall into the fill in the longitudinal direction after gap closure (Aviram et al. (2008), Mitoulis (2012)). The passive backfill behavior after failure of a sacrificial backwall has been supported by experimental studies (Romstad et al. (1995), Lemnitzer et al. (2009)). More recent studies investigated the shear key, wingwall, and transverse abutment behaviours and how shear key modelling assumptions impact bridge demands (Goel and Chopra (2008), Omrani et al. (2015), Kaviani et al. (2012)). The latter two studies also compared modelling assumptions on bridge demands for the case of straight vs skewed bridges. Skew bridges are particularly susceptible to gap closure and mobilization of abutment resistance mechanisms due to in-plane rotation of the superstructure (Meng et al. (2001)), differential contact occurring at the acute corners, and friction sliding when bridge longitudinal motion occurs. Maragakis and Jennings (1987) found considerable transverse displacements at the end supports as a result of rotations caused by deck-abutment interaction, rather than nonsymmetric restorative properties of the substructure or impact between deck and wing walls. Dimitrakopoulos (2011) emphasised the tendency of skew bridges to exhibit transverse displacements and

rotate after deck-abutment collisions is due to the planar geometry plus friction, not the skew angle alone. The research also reveals that the coupling between transverse displacements and rotations is stronger in the low frequency band of the spectrum, where contact is more intense and/or frequent. Bignell et al. (2005) found that the ultimate load capacity of a bridge is reduced by about two-thirds owing to the skew angle when compared to the corresponding non-skew bridge. Additional shear demands on the bearings were found to increase their failure risk, as found in skew impacts for multi-span simply supported bridges by Saadeghvaziri and Yazdanimotlagh (2008). The vulnerability of skew bridges motivated a large-scale experimental program that studied the effect of gap size, ground motion type and intensity (near and far field), and input excitation directions on displacements, rotations, and impact forces (Wu et al. (2019)). For modelling impacts in OpenSees, there exist several gap-contact elements (such as *ZeroLengthImpact3D*, *ZeroLengthContact*, *ZeroLengthInterface2D*) that have been introduced over the years, some of which have been applied to bridge abutment problems. Although there potentially remain benefits in new formulations or implementation of new elements (whether in commercial or open-source software), another option entirely is to use existing software, formulations, and elements to solve more complex or case-specific problems. Here we propose to use such an approach based on run-time user-driven parameter updates to solve the problem of contact-friction at bridge abutments. Parameters are a method of associating a pointer to a quantity of interest in the finite element domain, as first described in Scott and Haukaas (2008). Quantities of interest are typically model inputs such as nodal geometry, element or material properties, and load patterns, or model outputs such as nodal displacements, element forces, etc. Historically, parameters have been used for conducting (sequential) probabilistic simulations or material stage updating for geomechanics models. The concept of (potentially continuous) updating during the analysis was performed by Khorasani et al. (2015) for reliability analysis for fire loads and Whyte et al. (2016) for thermomechanical hybrid simulation. However, the first solution of more complex nonlinear responses using run-time model updating of parameters (without any new source) was performed by Rahman and Mackie (2023) to solve contact-friction problems. The latter formulation and implementation serves the basis for the abutment implementations presented in the present paper. The paper focuses on development and validation of the method for bridge abutment applications, followed by some preliminary analysis results for non-skewed bridges as part of a larger research effort on the effect of boundary conditions on different bridge configurations.

2. Contact-friction using parameter updates

2.1. Review of 2D contact using parameters

The proposed model by Rahman and Mackie (2023) is illustrated in Figure 1 for the response of a single unit process connecting two nodes using a local (possibly inclined) coordinate system. The local axis of the element is defined by the corresponding outward normal vector that describes the contact plane (y axis in Figure 1). This unit configuration can be replicated as many times as necessary to generate more complex contact-friction interfaces (node A need not be connected to fixity). The model is more easily visualized with an element of finite vertical dimension (labelled with the initial gap shown in the figure); however, nodes A and B may have the same nodal geometry (zero gap). The implementation in OpenSees is based on parameterization of existing *zeroLength* elements and constitutive models (*ElasticMaterial*, *ElasticPP*, *ElasticPPGap*); therefore, does not require any additional source code. Parameter updates occur entirely through the interpreter used to make the model input file. Therefore, the unit process behaviour can be integrated readily into existing models users have already developed. It will be demonstrated below that if the initial gap is zero, the formulation reproduces a node-to-node dry friction contact, whereas if the initial gap is greater than zero, the formulation reproduces a node-to-line (in 2D) or node-to-surface (in 3D) interface.

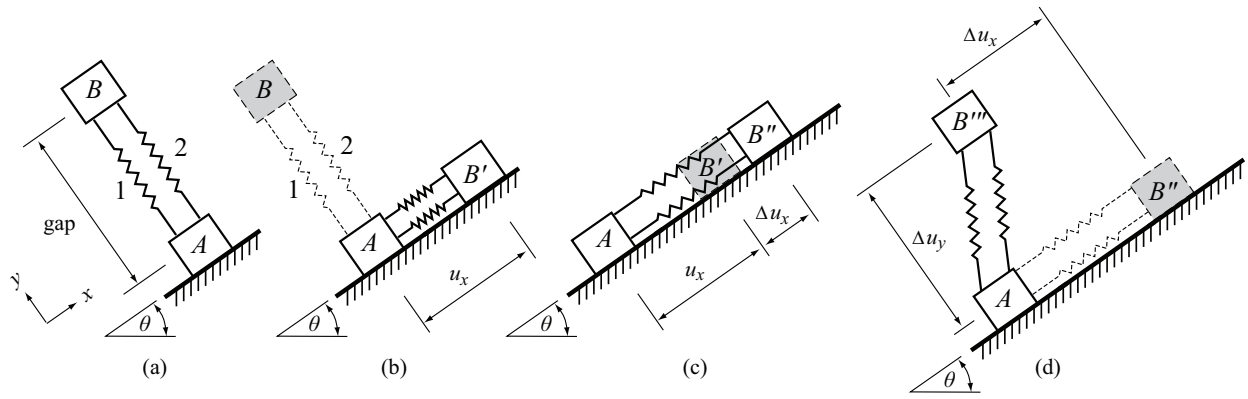

Figure 1: Illustrations of node-to-node contact friction behaviour in a local coordinate system as modelled by parameter updates.

The properties of the model are the gap and normal stiffness K_n for element 2, and the constant cohesion c, coefficient of static friction μ_s, and tangential stiffness K_t for element 1. The numerically large normal and tangential stiffness values are penalties for enforcing displacements where contact and slip occur, respectively, and are consistent with other contact-friction implementations. For the case of elasto-plastic constitutive models used in this paper (*ElasticPP* and *ElasticPPGap*), the parameters of the model are the modulus K_t and yield force $F_{\max}$ of element 1, and the modulus K_n of element 2. Although the contact-

friction problem can also be solved using only *ElasticMaterials*, it requires internal tracking of the stick point (denoted s_x and s_y for each local axis, respectively) in the model that can change during the analysis.

2.2. Extension to 3D contact

The abutment (and bridge) modelling needs are for 3D elements, so it was necessary to extend the 2D unit process from Rahman and Mackie (2023) to the 3D case here. However, the 3D case is also easily treated using parameters. The additional quantities for displacement and force in the local z-axis are necessary, and correspond to an additional element 3. A schematic of the two node unit process in the local coordinate system (here shown horizontally but can be defined by arbitrary direction cosines) is shown in Figure 2. Methodologically, an additional step is necessary to resolve the maximum frictional force $F_{\max}$ into F_x and F_y (local axis z is considered the outward normal). The orientation of the in-plane friction vector was obtained using the direction cosines of the relative (to the stick point) in-plane displacements. This guarantees $F_{\max}$ is the maximum achievable resistance regardless of the in-plane direction of load. Note this also guarantees there is coupling between elements 1 and 2 (although they are individual elements in the finite element domain).

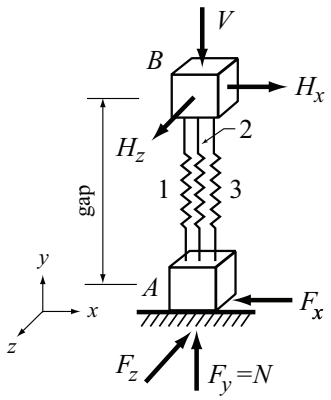

Figure 2: Two node unit process in three-dimensional contact-friction model.

Figure 3 shows the response of a 3D unit process due to two horizontal displacements (x and y) and one vertical (z) displacements. The vertical displacement is a square wave, which determines the contact between the nodes, having period of 2.5 s and amplitude of 0.1 m. The two out-of-phase horizontal displacements are both triangular waves having period of 4 s and 6 s with amplitude of 1 m and 2 m respectively. The friction coefficient μ_s is 0.3 and the cohesion is 1500 N.

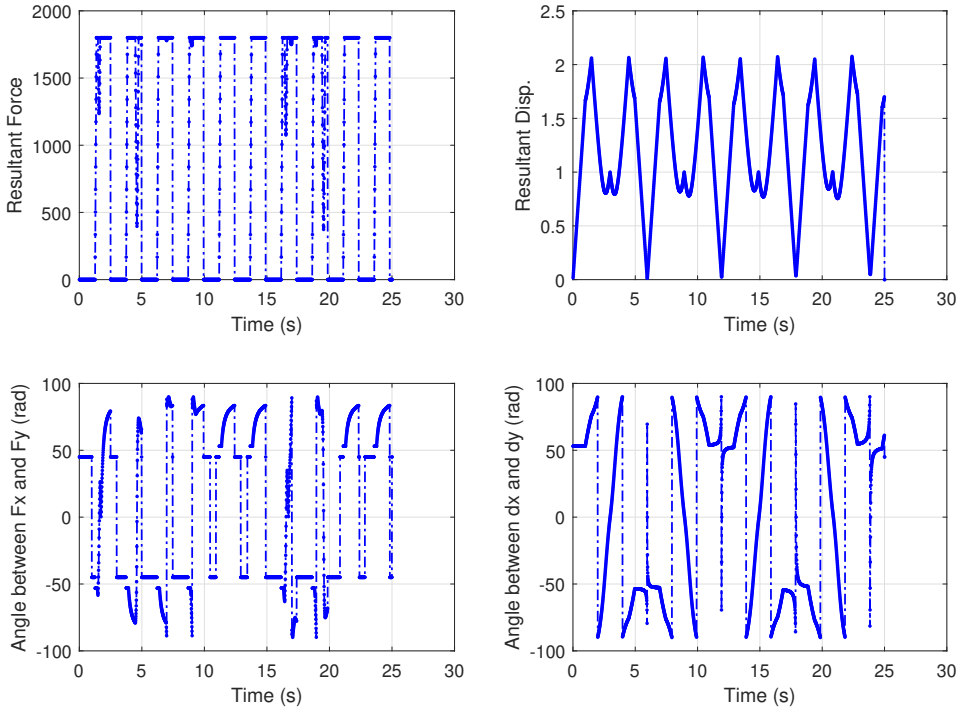

Figure 3: Response of 3D unit process under out-of-phase horizontal and vertical displacements.

2.3. Visualizing node-to-line in 2D

Although the method is a node-to-node method (there is an element connecting two pre-existing nodes that have an initial gap or not), it behaves like a node-to-line (in 2D) contact interface due to the calculation of the perpendicular distance to the line (i.e., local coordinate system x-axis). The extension to node-to-surface is also true of the 3D case, as necessitated by the abutment interaction interfaces. As an illustration of the phenomenon in 2D, the nonlinear dynamic response of a single mass is investigated using two inclined unit processes (with gaps of opposite signs). Figure 4 shows the response of a node moving in a two-dimensional space under dynamic loads. The movement of the node is bounded by two inclined surfaces at 30 degrees, as shown by the green and blue lines. The perpendicular distance from the reference line (shown in black) to either of the surface is 0.0268 m. The input acceleration is a cosine pulse of 0.5 s period with amplitude of 0.5 g in the horizontal direction and 1.5 g in the vertical direction. The friction coefficient μ_s is 0.1, cohesion is negligible and the damping ratio is 5%. From the element deformation plots, it can be observed that the normal displacements are bounded by the perpendicular distance of 0.0268 m for both elements, as expected.

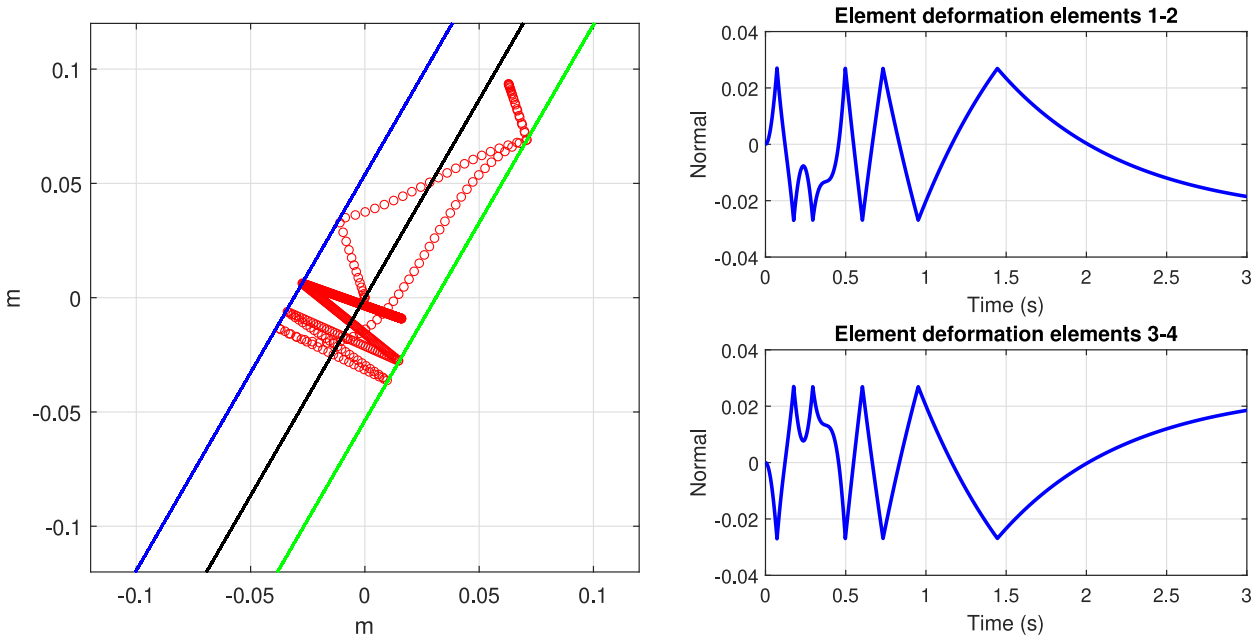

Figure 4: Two-dimensional particle under dynamic excitation bounded by two lines.

3. Verification Case Studies

Before deploying the parameter-based contact friction model in the 3D abutment and bridge models, the planar responses of simplified skew bridge abutment systems were compared with the response histories of two other studies from the literature. One study is an idealized numerical model that uses linear complementarity for contact and detachment (Dimitrakopoulos (2011)), whereas the second study is a large set of experimental shake table studies conducted with impacts (Wu et al. (2019)).

3.1. Dimitrakopoulos

The seismic behaviour of short skewed bridges with deck-abutment joints was studied by Dimitrakopoulos (2011). It provides an event-based, non-smooth dynamics method to seismic response analysis, and it uses formal dimensional analysis to characterise similarity in bridge responses. The contact between skewed bridges and joints is modelled as a linear complementarity problem (LCP) for continuous contact and detachment. The study focuses on a specific skew bridge segment with length and breadth of 30m and 15m, respectively, with skew angles ranging from 20 to 60 deg. The base excitation was a cosine pulse along the longitudinal axis. Transverse displacements and rotations in skewed bridges following deck-abutment collisions were shown to depend on not only the skew angle, but also by the bridge's plan geometry and friction. The coupling effect was particularly evident in the low-frequency spectrum and results in novel dimensionless response spectra for these oblique contact displacements and rotations.

For the case of $W/L = 1/2$, $\alpha = 30$ deg, dimensionless gap 0.1, $\mu_s = 0$, and $a_p = 0.5$ g, the parameter updating approach was used to model the same setup. The deck consisted of perimeter *elasticBeamColumn* elements of high stiffness, whereas the unit contact-friction process was deployed at each contact location (with outward normal vector pointing away from the boundary toward the bridge deck). Cohesion and μ_s were set to zero and $K_n = 1.0\text{e}7$ N/m. To address the high frequency content generated as a result of impact, the linear multistep method of Houbolt was used in the OpenSees analysis. Comparisons of the time-dependent displacements in the global x and y directions, and the center of mass rotation are shown in Figure 5. The Newmark solution is the uncoupled solution (solution without impacts) using the standard Newton integrator.

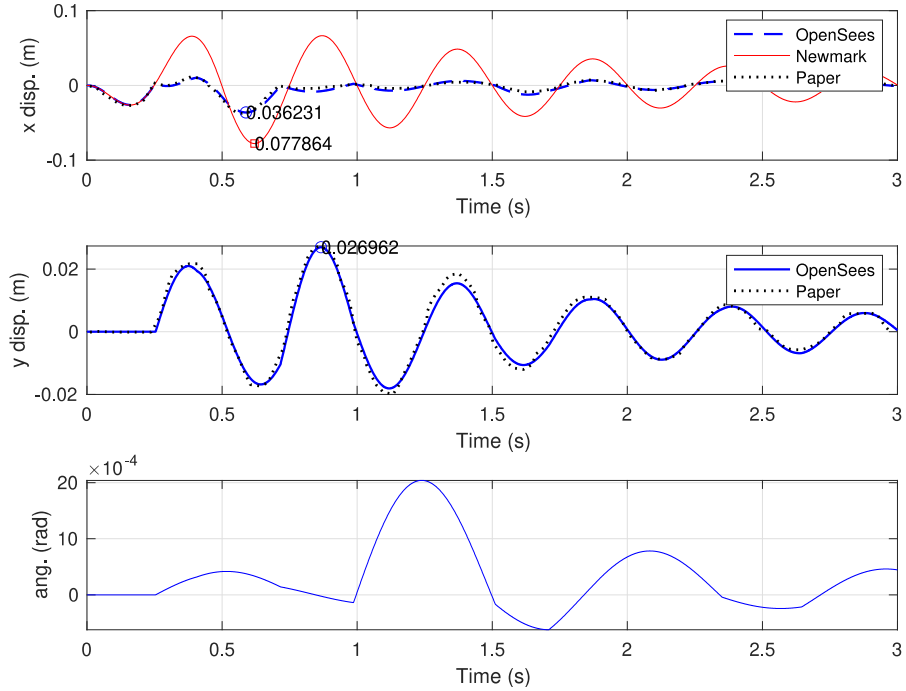

Figure 5: Comparison of OpenSees parameter updating displacement solution with Figure 6 (right) from Dimitrakopoulos (2011).

The relative tangential and normal displacements at the locations g_{N1} and g_{N2}, as denoted in the original paper, are shown in Figure 6. OpenSees elements 1-2 correspond to the location g_{N2}. The center of mass displacements agree between the two methods; however, there are slight differences evident in the phase-amplitude relationship over time as the number of impacts increases. This is due to the numerical implementation of contact (with a finite penalty) and the lack of a formal coefficient of restitution in the numerical model. The actual coefficient of restitution measured was between 0.45 (large contact velocity) to 0.71 (small contact velocity). The differences can be mitigated by using a K_n value that depends on the

approach velocity or a viscous damper, both of which are readily implementable in the parameter updating framework; however, was not performed here.

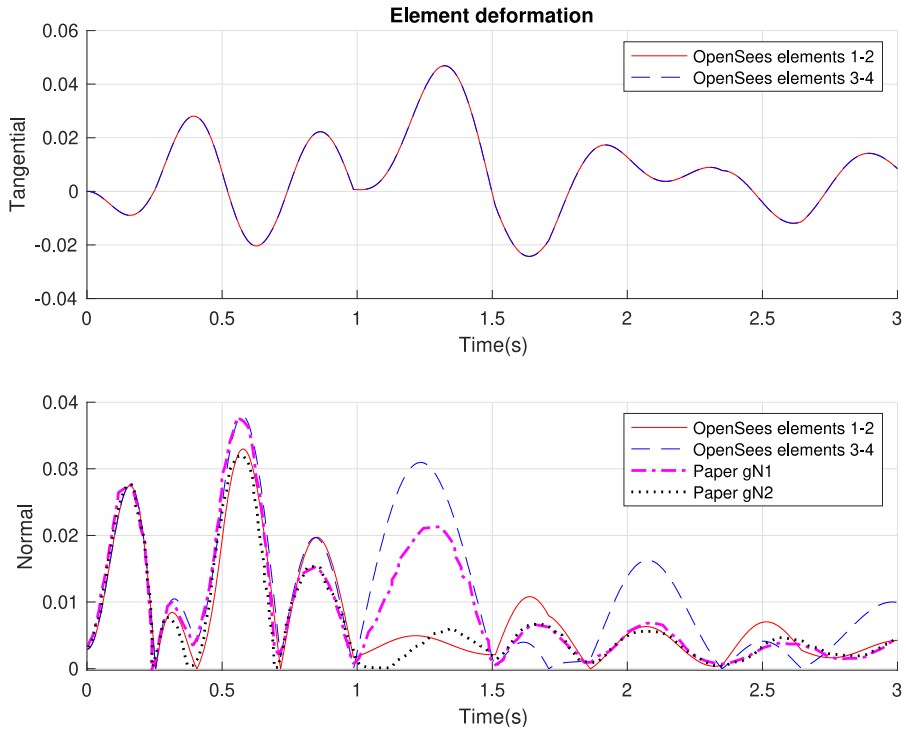

Figure 6: OpenSees tangential and normal displacement components at the impact locations compared with Dimitrakopoulos (2011) Figure 6 (right).

3.2. Wu

The paper describes an experimental study that investigated the impact between skewed bridge superstructures and seat-type abutments. Four separate single-span, simply-supported bridges with variable lengths (ranging from 3.2 m to 5.03 m) and a width of 1.07 m were used in the shake table runs. The skew angles of these models were 0, 30, 45, and 60 deg, and the study looked at five different expansion gaps ranging from 0 to 6.35 mm. The models were subjected to recorded El Centro 1940, Century City 1994, and Sylmar 1994 motions, with intensity levels ranging from 50% to 200%, and components of motion applied along one or both bridge axes. Superstructure displacements and accelerations, as well as impact forces at the abutments, were all recorded. The findings revealed that when a skewed bridge's obtuse corner collides with the neighbouring rear wall, with or without slippage, the bridge undergoes considerable in-plane rotation. As a result, these bridges can experience significant in-plane displacements perpendicular to the back wall at their acute corners, requiring longer support lengths to avoid unseating than straight bridges.

The cases of $W = 1.07$ m, $L = 5.03$ m, $\alpha = 60$ deg, 100% of design earthquake using El Centro (bidirectional case), and gaps of 3.18 mm (run 123) and 6.35 mm (run 213) were used. The properties of the bearings (both stiffness and equivalent viscous damping) and the coefficient of static friction (0.4) were derived from the information in the paper. The model used $K_n = 2.0$e7 N/m and zero cohesion. The comparison of tangential and normal element deformations at the four corners are shown in Figure 7 for a subset of the ground motion excitation time. Note, it is not known exactly what the ground motion acceleration input was; however, the normal deformations have similar phasing and amplitude. Immediately following contact there is some loss in coherence that could be related to the assumed K_n and μ_s, velocity and amplitude-dependent damping, and nonlinear elastic bearing response.

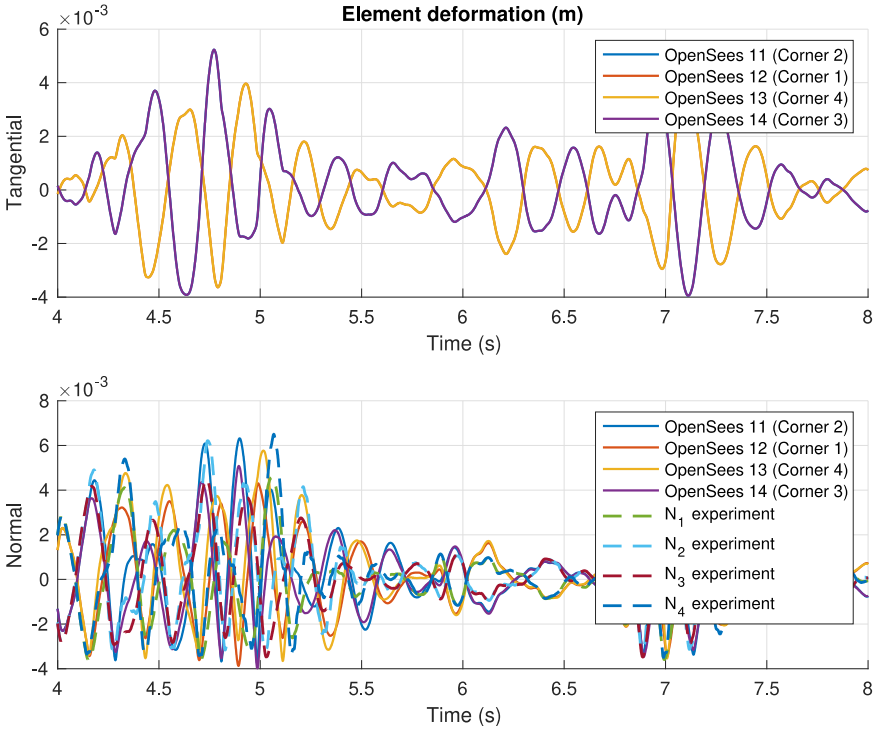

Figure 7: Element deformation time histories compared with experimental results in Wu et al. (2019) for run 123.

The forces mobilized in the tangential (friction) and normal directions are shown in Figure 8. Due to the compliance of the impacts, the contact time and time to mobilize the peak frictional response are longer than those presented in the Dimitrakopoulos example. The relative ordering of impact forces at the opposite corners is consistent with the experimental load cell readings; however, the magnitudes are as much as 50-100% different.

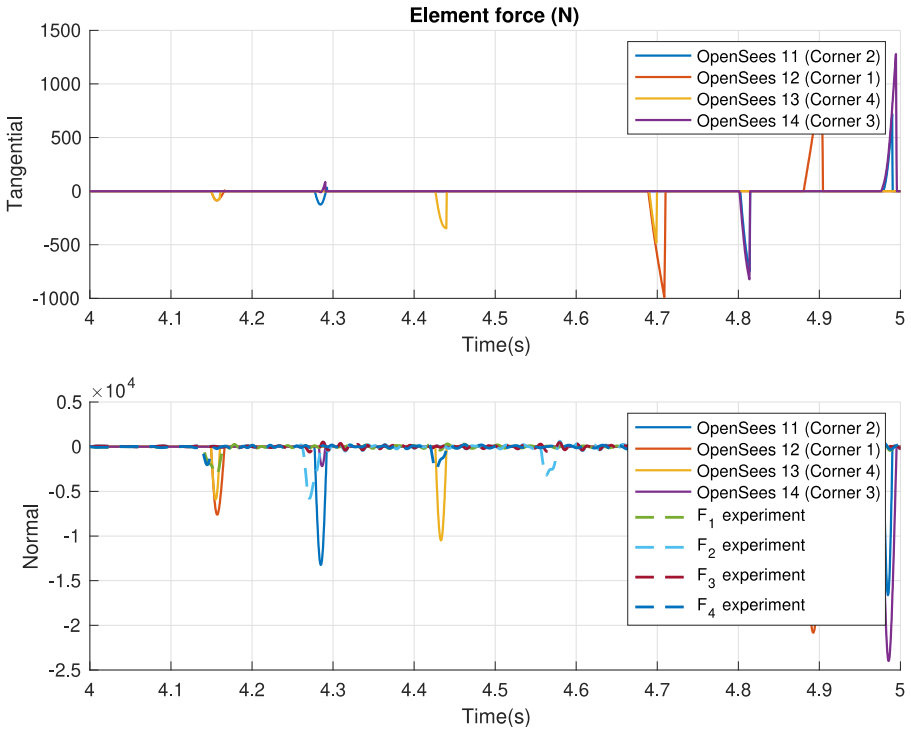

Figure 8: Element force time histories compared with experimental results in Wu et al. (2019) for run 123.

4. Full-scale abutment model

The contact abutment model is a three-dimensional representation of the structural components of the abutment that surround the end diaphragm. The model uses one-dimensional elements for all of its components. The abutment, which shown in Figure 9, the three transverse arrays of stiff elastic elements correspond to the edges and centerline of the seat. These elements use a large displacement transformation (corotational). The centerline array is used to connect the bearings, modelled using plasticity-based elastomeric bearings (*elastomericBearingPlasticity* in OpenSees). This enables P-Delta effects and nonlinear hardening. The behaviours of the exterior shear key, backwall, wingwall, and backfill are assumed to be the same as in previous studies (Mackie and Scott (2020); Aviram et al. (2008); Mackie et al. (2017)). The vertical separation between the arrays is a finite length defined by the height of the bearings (this is exaggerated in the figure), not the height of the back wall. Rotation about the transverse axis of the arrays is constrained. A physical separation between the final transverse array at deck level and the back wall, shear key assembly (shown in blue) corresponds to the longitudinal and transverse gaps.

The nonlinear static response of the contact-friction abutment, where friction does not contribute due to lack of skew and displacements imposed along principal abutment axes independently, are the same as

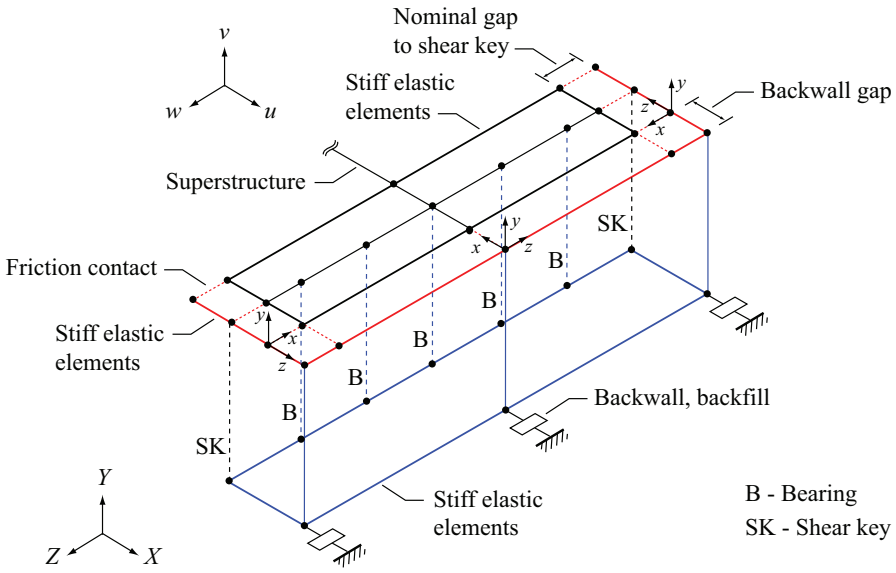

Figure 9: Schematic of contact-friction abutment model (dotted red lines indicate contract-friction elements).

those shown in Mackie and Scott (2020) and not repeated here. Initial gaps of 5.1 cm and 0.64 cm were assumed in the longitudinal and transverse directions, respectively. To compare the response histories with and without the presence of friction ($\mu_s = 0.5$ and 0, respectively), the Northridge TAR (Tarzana – Cedar Hill) ground motion was applied to the abutment substructure (with only a nodal mass at the connector node). The 000 component was applied along the local w axis, while the 090 component was applied along the local u axis. A skew angle of $\alpha = 25$ deg was used in the full-scale abutment examples.

The hysteretic responses in each primary abutment axis are compared with and without friction in Figure 10. Note there is no frictional sliding due to longitudinal motion (abutment is not skewed); therefore, there is minimal effect of the frictional force on the longitudinal response. Small amplitude, high frequency vibrations are evident in the longitudinal hysteresis (due to stick-slip events taking place with shear keys due to smaller gaps on both sides as superstructure moves longitudinally). The differences in the transverse direction are more pronounced and represent the frictional force mobilized parallel to the back wall. Multiple frictional contacts occur when longitudinal gap closure occurs, with the resulting reduction in the peak transverse displacements during multiple cycles

5. Bridge response history analysis

The effect of contact-friction at the abutments was extended to the bridge system level with response history analysis. Two of the Ordinary Standard Bridges (OSBs) developed for several previous studies were

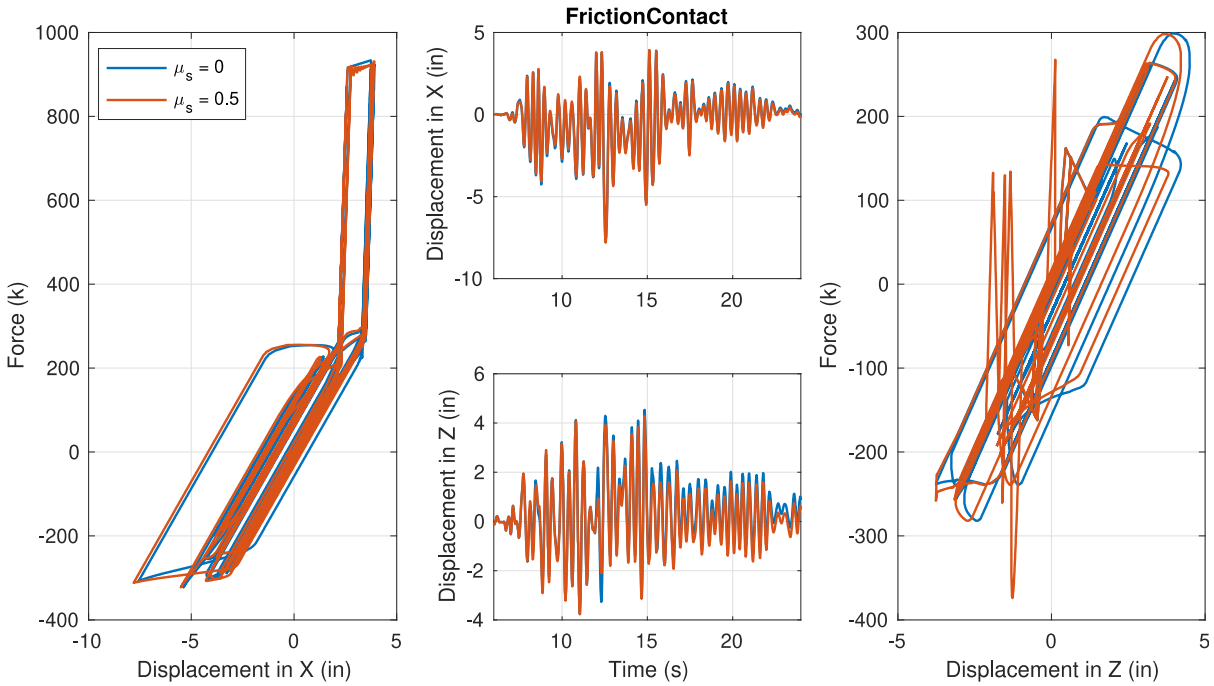

Figure 10: Nonlinear dynamic response of abutment subsystem subjected to TAR ground acceleration.

employed here, specifically OSB1 and OSB2 that are both monolithic reinforced concrete bridges with seat-type abutments. The 3D bridge models were created previously (Mackie and Scott (2020)) with the variant developed in OpenSees that utilized distributed plasticity force-based column models used here. Note the Mackie and Scott (2020) bridge analyses used only contact, not contact-friction. OSB1 is a two-span concrete bridge with a single two-column bent at the center. The clear column height is 5.64 m. Each span is 45.7 m long. The bent contains two 1.68 m diameter circular reinforced concrete columns at 7.32 m (center-to-center) spacing.

Two orthogonal horizontal components of recorded ground motion accelerations were used in all response history analyses. In the case of the bridge models, the Loma Prieta WAH (WAHO station) record was used with components 000 and 090 applied in the transverse and longitudinal bridge directions, respectively. The vertical ground acceleration input was not included in the current analysis. Nonlinear time history analysis was conducted for all abutment-bridge-ground motion combinations using the Houbolt integrator and step size of 0.005 s. Rayleigh damping was used with a mass and stiffness proportional term taken from previous studies (Mackie et al. (2017)). Only a small selection of bridge results are presented here.

The comparison of center of mass displacement time histories (with and without friction) for the bridge

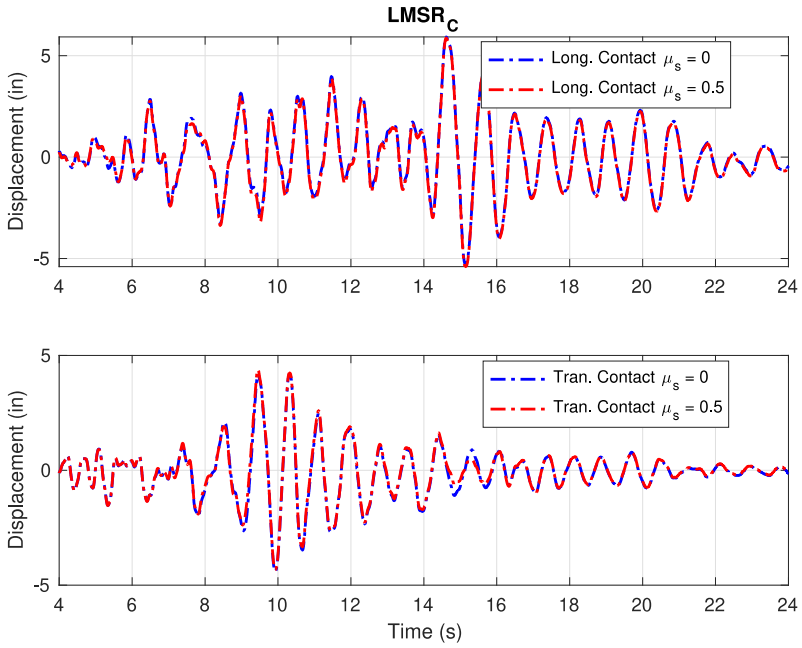

Figure 11: Bridge center of mass displacement histories for bridge OSB1 under ground motion WAH.

are shown in Figure 11. The left and right abutment hystereses are shown in Figure 12. As with the abutment-only responses, the frictional forces reduce the peak displacement amplitudes in cycles with contact. Due to the non-skewed bridge, the friction-contact is most visible in the transverse hysteresis due to back wall friction that occurs with transverse movement and gap closure. The result of friction is a coupling of the longitudinal and transverse directions of response, even in the absence of skew. Therefore, the peak displacement demand was reduced only 2-3% and the column shear demand a similar amount. Far larger differences can be observed during cycles in which the significant displacement excursions in the longitudinal and transverse directions are in phase.

6. Discussion and conclusions

This paper demonstrated the application of user-driven run-time parameter updates to solve the contact-friction behaviors occurring in bridge seat-type abutments. The major benefit was the implementation used only zeroLength elements and elastic-plastic or elastic-plastic-gap materials in OpenSees (no new source code necessary). Calibration of the 2D and 3D behaviors of the implementation (including node-to-line or node-to-surface behaviors) were presented, followed by comparison with 2D skewed bridge results from both the analytical and experimental literature. Nonlinear static behaviors of the previously developed Spring and Contact-Friction were extended to nonlinear dynamic cases that included cohesion and friction.

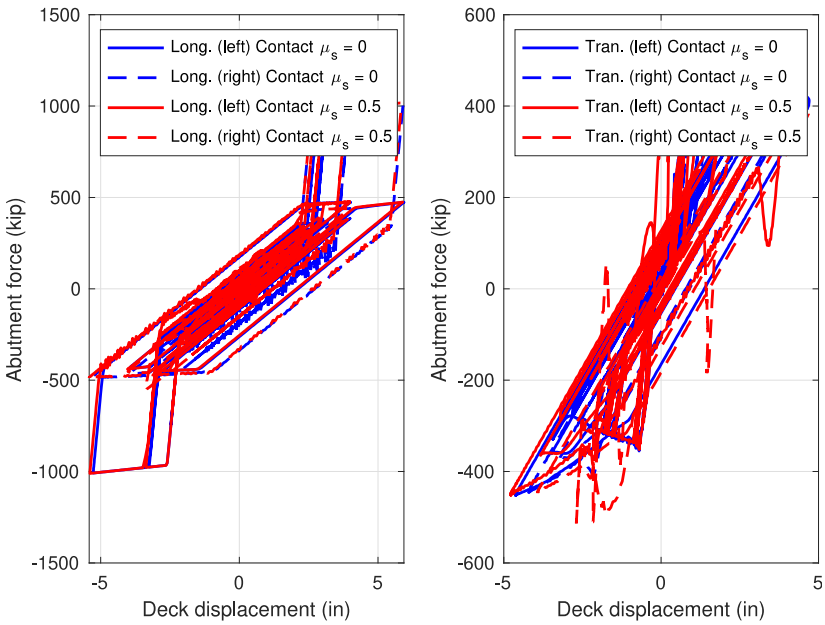

Figure 12: Left and right abutment hysteresis for bridge OSB1 under ground motion WAH.

Finally, preliminary results from a larger research program on bridge boundary conditions were presented considering non-skewed bridges studied in previous projects.

Results showed coupling between primary bridge directions when friction was considered. However, only small differences were observed in peak bridge demands. The models will be extended to more bridge and abutment configurations, skew angles, and larger ground motion ensembles in future work. While there are ostensible behavior observations that can be drawn from the above studies, an additional dimension to the parameter-based implementation is it facilitates solution of more complex interactions. Examples include nonlinear penalties in the normal and tangential directions, control of stiffness and damping terms to elicit amplitude-dependent coefficients of restitution, and more general advances in tribology studies such as non-Coulomb interfacial laws. Similarly, parameterization allows study of multi-physics problems with one-way coupling such as mechanics with temperature degrees of freedom, or time dependent concrete creep and shrinkage.

References

K. R. Mackie, M. H. Scott, K. Johnson, M. Al-Ramahee, M. Steijlen, Nonlinear Time History Analysis of Ordinary Standard Bridges, Technical Report 17-65A0559, California Department of Transportation, Sacramento, CA, 2017.

A. Aviram, K. R. Mackie, B. Stojadinovic, Guidelines for Nonlinear Analysis of Bridge Structures in California, Technical Report 2008/03, Pacific Earthquake Engineering Research Center, Berkeley, CA, 2008.

A. Shamsabadi, M. Ashour, G. Norris, Bridge abutment nonlinear force–displacement–capacity prediction for seismic design, Journal of Geotechnical and Geoenvironmental Engineering 131 (2005) 151–161.

A. Sextos, K. Mackie, B. Stojadinovic, O. Taskari, Simplified py relationships for modelling embankment abutment systems of typical california bridges, in: Proceedings of the 14th World Conference on Earthquake Engineering, Beijing, China, 2008.

O. Taskari, A. Sextos, Stiffness and ultimate capacity of typical abutment–embankment systems, in: Proceedings of the 15th World Conference on Earthquake Engineering, Lisbon, Portugal, 2012.

H. H. Darwash, K. R. Mackie, Effect of seat-type abutment load path and failure mode on seismic response of straight ordinary bridges, Engineering Structures 242 (2021) 112560.

M. Inel, M. A. Aschheim, Seismic design of columns of short bridges accounting for embankment flexibility, Journal of Structural Engineering 130 (2004) 1515–1528.

A. Kotsoglou, S. Pantazopoulou, Response simulation and seismic assessment of highway overcrossings, Earthquake Engineering and Structural Dynamics 39 (2010) 991–1013.

J. C. Wilson, Stiffness of non-skew monolithic bridge abutments for seismic analysis, Earthquake Engineering and Structural Dynamics 16 (1988) 867–883.

J. Zhang, N. Makris, Kinematic response functions and dynamic stiffnesses of bridge embankments, Earthquake Engineering and Structural Dynamics 31 (2002).

S. A. Mitoulis, Seismic design of bridges with the participation of seat-type abutments, Engineering Structures 44 (2012) 222–233.

K. Romstad, B. Kutter, B. Maroney, E. Vanderbilt, M. Griggs, Y. H. Chai, Experimental Measurements of Bridge Abutment Behavior, Technical Report UCD-STR-95, University of California, Davis, 1995.

A. Lemnitzer, E. R. Ahlberg, R. L. Nigbor, A. Shamsabadi, J. W. Wallace, J. P. Stewart, Lateral performance of full-scale bridge abutment wall with granular backfill, Journal of Geotechnical and Geoenvironmental Engineering 135 (2009) 506–514.

R. K. Goel, A. K. Chopra, Role of shear keys in seismic behavior of bridges crossing fault-rupture zones, Journal of Bridge Engineering 13 (2008) 398–408.

R. Omrani, B. Mobasher, X. Liang, S. Gunay, K. M. Mosalam, F. Zareian, E. Taciroglu, Guidelines for nonlinear seismic analysis of ordinary bridges: Version 2.0, Caltrans Final Report (2015).

P. Kaviani, F. Zareian, E. Taciroglu, Seismic behavior of reinforced concrete bridges with skew-angled seat-type abutments, Engineering Structures 45 (2012) 137–150.

J. Y. Meng, E. M. Lui, Y. Liu, Dynamic response of skew highway bridges, Journal of Earthquake Engineering 5 (2001) 205–223.

E. A. Maragakis, P. C. Jennings, Analytical models for the rigid body motions of skew bridges, Earthquake Engineering and Structural Dynamics 15 (1987) 923–944.

E. G. Dimitrakopoulos, Seismic response analysis of skew bridges with pounding deck–abutment joints, Engineering Structures 33 (2011) 813–826.

J. Bignell, J. Lafave, N. Hawkins, Seismic vulnerability assessment of wall pier supported highway bridges using nonlinear pushover analyses, Engineering Structures 27 (2005) 2044–2063.

M. Saadeghvaziri, A. Yazdanimotlagh, Seismic behavior and capacity/demand analyses of three multi-span simply supported bridges, Engineering Structures 30 (2008) 54–66.

S. Wu, I. G. Buckle, A. M. Itani, D. Istrati, Experimental studies on seismic response of skew bridges with seat-type abutments. ii, Journal of Bridge Engineering 24 (2019).

M. H. Scott, T. Haukaas, Software framework for parameter updating and finite-element response sensitivity analysis, Journal of

Computing in Civil Engineering 22 (2008) 281–291.

N. Khorasani, M. Garlock, S. Quiel, Modeling steel structures in opensees: Enhancements for fire and multi-hazard probabilistic analyses, Computers and Structures 157 (2015) 218–231.

C. A. Whyte, K. R. Mackie, B. Stojadinovic, Hybrid simulation of thermomechanical structural response, Journal of Structural Engineering 142 (2016).

A. Rahman, K. R. Mackie, Node-to-node contact-friction problems using run-time parameter updates on a conventional force–deformation finite element, Finite Elements in Analysis and Design 218 (2023).

K. R. Mackie, M. H. Scott, Extending bridge modeling to include changes in the vertical system for collapse simulation, in: Proceedings of the 17th World Conference on Earthquake Engineering, Santiago, Chile, 2020.